Excitatory monocyte chemoattractant protein-1 signaling is up-regulated in sensory neurons after chronic compression of the dorsal root ganglion

Fletcher A. White*†‡, Jihu Sun§, Stephen M. Waters¶, Chao Ma§, Dongjun Ren‖, Matthew Ripsch*, Jeremy Steflik¶, Daniel N. Cortright¶, Robert H. LaMotte§, and Richard J. Miller‖

Departments of *Cell Biology, Neurobiology, and Anatomy, and †Anesthesiology, Stritch School of Medicine, Loyola University Chicago, Maywood, IL 60153; ¶Neurogen Corporation, Branford, CT 06405; §Department of Anesthesiology, Yale University School of Medicine, New Haven, CT 06510; and ‖Department of Molecular Pharmacology and Biological Chemistry, Feinberg School of Medicine, Northwestern University, Chicago, IL 60611

Edited by Solomon H. Snyder, Johns Hopkins University School of Medicine, Baltimore, MD, and approved July 29, 2005 (received for review April 27, 2005)

Neuronal hyperexcitability in both injured and adjacent uninjured neurons is associated with states of chronic injury and pain and is likely subject to neuroinflammatory processes. Chronic inflammatory responses are largely orchestrated by chemokines. One chemokine, monocyte chemoattractant protein-1 (MCP-1), in the presence of its cognate receptor, the β chemokine receptor 2 (CCR2), produces neural activity in dissociated neuronal cultures of neonatal dorsal root ganglion (DRG) neurons. Using a neuropathic pain model, chronic compression of the DRG (CCD), we compared anatomically separate populations of noncompressed lumbar DRG (L3/L6) with compressed lumbar DRG (L4/L5) for changes in the gene expression of CCR2. *In situ* hybridization revealed that CCR2 mRNA was up-regulated in neurons and nonneuronal cells present in both compressed L4/L5 and ipsilateral noncompressed L3/L6 DRGs at postoperative day 5 (POD5). The total percentages of compressed and noncompressed neurons exhibiting CCR2 mRNA transcripts in L3, L5, and L6 DRG were 33 ± 3.5%, 49 ± 6.2%, and 41 ± 5.6%, respectively, and included cell bodies of small, medium, and large size. In addition, the preferred CCR2 ligand, MCP-1, was up-regulated by POD5 in both compressed L4/L5 and noncompressed L3/L6 DRG neurons. Application of MCP-1 to the cell bodies of the intact formerly compressed DRG *in vitro* produced potent excitatory effects not observed in control ganglia. MCP-1/CCR2 signaling is directly involved with a chronic compression injury and may contribute to associated neuronal hyperexcitability and neuropathic pain.

hyperalgesia | nerve injury | neuropathic pain | peripheral sensitization

Inflammation accompanying peripheral nerve injury frequently produces neuropathic pain symptoms, such as hyperalgesia and allodynia. This hyperalgesia may reflect ongoing or ectopic changes in the excitability of neurons in both injured and adjacent uninjured dorsal root ganglion (DRG) (1). Mechanisms that may contribute to the changes in neuronal activity include altered expression of ion channels, kinases, enzymes, neuropeptides, transcription factors, neurotrophins, and/or the *de novo* presence of proinflammatory mediators such as cytokines, chemokines, and their respective receptors. However, current knowledge of the modification of molecular properties in both injured and noninjured adjacent ganglia is limited.

Recent studies implicate the β chemokine receptor 2 (CCR2) in the development and maintenance of pain (2–4). CCR2 is a G protein-coupled receptor that is related in structure to other CCRs (5, 6) and is largely thought to be a major regulator of induced macrophage migration (7–9). CCR2 is also constitutively expressed by different types of cells in the central nervous system, including neurons (10, 11), activated astrocytes (12, 13), microglia (3), and neural progenitor cells (14, 15).

Most CCRs, including CCR2, bind multiple chemokines (16, 17). CCR2 binds a family of closely related β-chemokines (C-C) called monocyte chemoattractant proteins (MCP), of which there are five members, MCP1–5 (also known as CCL2, CCL8, CCL7, CCL13, and CCL12, respectively). All members of this C-C family of chemokines exhibit chemotactic effects on leukocytes in a number of disease processes. However, evidence obtained from studies on leukocytes suggest the chemokine MCP-1 preferentially binds to CCR2 (18). MCP-1 also binds to the orphan chemokine-like receptor L-CCR (19) and a nonsignaling decoy receptor, D6 (20), which may act as a inflammatory chemokine scavenger.

MCP-1 is not expressed at high levels in the normal nervous system, although its synthesis can be significantly up-regulated in response to different types of injury. For example, expression of MCP-1 can be induced by nerve injury (21, 22), possibly in response to upstream regulators such as IL-6, leukemia inhibitory factor (23), or NF-κB (24).

Here we analyzed changes in gene expression associated with a rodent model of neuropathic pain, a chronic compression of the DRG (CCD) (25–27) by using *in situ* hybridization. We examined gene regulation of CCR2 and protein expression of MCP-1 in sham, injured, and adjacent uninjured ganglia, as potential mediators of neuropathic pain in CCD. We further evaluated the role of CCR2 and MCP-1 in the CCD model by using intracellular electrophysiology. Our findings further implicate MCP-1/CCR2 signaling in the maintenance of neuropathic pain and suggest that CCR2 may be a therapeutic target for this disorder.

Materials and Methods

Animals. Fifty female Sprague–Dawley rats (Charles River Breeding Laboratories) weighing 150–200 g at the time of testing were maintained in a climate-controlled room on a 12-h light/dark cycle (lights on at 0600) with food and water available *ad libitum*.

Chronic Compression of the DRG. A full description of the model and surgical procedure is available elsewhere (26). Briefly, after anesthesia with pentobarbital sodium (40 mg/kg, i.p.), the paraspinal muscles were separated from the mammillary and transverse processes to expose the intervertebral foramina at lumbar DRG (L)4 and L5. A sharp stainless steel needle, 0.4 mm in diameter with a right angle to limit penetration, was inserted ≈4 mm into the foramen at L4 and again at L5 in a rostral direction (≈30–40° angle) to the dorsal middle line and −10° to −15° below the vertebral horizontal line (25). After ≈1 s, the

This paper was submitted directly (Track II) to the PNAS office.

Abbreviations: DRG, dorsal root ganglion; CCR2, β chemokine receptor 2; MCP, monocyte chemoattractant protein; L*n*, lumbar DRG *n*; CCD, chronic compression of the DRG; POD*n*, postoperative day *n*.

‡To whom correspondence should be addressed. E-mail: fwhite@lumc.edu.

www.pnas.org/cgi/doi/10.1073/pnas.0503496102

needle was withdrawn, and a stainless steel rod, L-shaped, 4 mm in length and 0.63 mm in diameter, was implanted into each foramen. Each rod was oriented in a manner described for the needle. After the rod was in place, the muscle and skin layers were sutured. An antibiotic, Baytril (enrofloxacin, 2.5 mg/kg i.m., Bayer HealthCare, Shawnee Mission, KS) was administered immediately after surgery. Sham-operated control rats underwent the same surgical procedure as described, except that each rod was withdrawn ≈1 s after insertion.

***In Situ* Hybridization of CCR2.** *In situ* hybridization histochemistry for CCR2 was performed by using digoxigenin-labeled riboprobes. L3–L6 DRGs ipsilateral to CCD injury were rapidly removed, embedded in OCT compound (Tissue Tek, Ted Pella, Inc., Redding, CA) and frozen. Sections were cut serially at 14 μm. Briefly, an 848-bp CCR2 cDNA fragment (nucleotides 489-1336 of GenBank no. U77349) was cloned by PCR by using rat spleen cDNA. The resulting PCR product was subcloned into pGEM-T Easy and sequenced to ensure identity for riboprobe use. CCR2 template was linearized with SacII to generate a probe of 950 bases by using SP6 polymerase. Signals were visualized by using NBT/BCIP reagents (Boehringer Mannheim) in the dark for 2–20 h depending upon the abundance of the RNA. The *in situ* image was captured by using a Retiga (Skokie, IL) EX charge-coupled devise camera. CCR2mRNA expression studies were used for receptor localization because of the failure of immunocytochemistry to detect neuronal CCR2 protein.

Immunocytochemical Labeling of Compressed and Adjacent Noncompressed DRG. Adult female Sprague–Dawley rats were deeply anesthetized with isoflurane and transcardially perfused with saline followed by 4% paraformaldehyde. L3–L6 ganglia ipsilateral to CCD injury were removed from rats at postoperative day 3 (POD3) ($n = 3$), POD5 ($n = 5$), and POD24 ($n = 2$) and from sham-injured rats ($n = 3$) at POD5 and postfixed for 4 h. Sections were cut serially at 14 μm and incubated with blocking buffer (3% BSA/3% horse or goat serum/0.4% Triton) for 1 h, followed by overnight incubation with the polyclonal antisera generated against MCP-1 (1:1,000; Chemicon, Temecula, CA) at room temperature. Macrophages were identified in the DRG by using the monoclonal antisera generated against monoclonal antibody clone ED-1 (1:1,000; Serotec). After primary incubation secondary antibodies (anti-mouse or -rabbit conjugated to CY3, made in horse or goat, respectively, at 1:1,000; Jackson ImmunoResearch) were used to visualize cells. Some experiments were augmented with the addition of *Bandeiraea* (*griffonia*) *simplicifolia* I-isolectin B4 (IB4) conjugated with fluorescein (1 mg/1 ml; Sigma). Slides were washed in PBS for 5 min each (×3) and coverslipped with PBS/glycerol solution. The signal from labeled cells was captured with a fluorescent microscope fitted with a charge-coupled device camera.

Neuronal Cell Counts. The numbers of CCR2-positive DRG neurons present in L3, L5, and L6 DRGs removed from CCD POD5 animals ($n = 4$) were derived from tissue cryosections processed for CCR2 *in situ* hybridization experiments. An observer blinded to the experiments evaluated the tissue sections by using the physical dissector method of cell counting (28), which provided unbiased estimates of single-labeled CCR2 DRG cell numbers. Briefly, pairs of tissue sections (84 μm apart, every sixth section) were digitally photographed and stored in eight-bit (256 level) format. Using PHOTOSHOP 5.5 (Adobe Systems, San Jose, CA), a density threshold was set to identify positive neuronal cells. Neuronal profiles with transcript densities at least four times higher than the background densities were considered positively labeled. A new image layer was established in PHOTOSHOP 5.5 on which all labeled cell profiles were outlined in addition to an appropriate number of fiduciary landmarks. The layers from each section pair were then matched with one another by using fiduciary landmarks, and all labeled profiles that appear in both sections were disallowed. The labeled profiles remaining were considered positive. The total number of labeled cells was estimated in each sampled section by using the fractionator principle, whereby counts from each pair of sections were summed and multiplied by section separation and by the reciprocal of the fraction of each sampled section and then divided by two (because double dissectors were used). At least five pairs of tissue sections were used for analysis from each individual ganglia.

After quantitative analysis of CCR2-positive neurons, coverslips were carefully removed and sections counterstained with cresyl violet. The total number of neurons was obtained by using pairs of sections in a fashion similar to the above description and a final percentage of CCR2-positive neurons determined.

In similar fashion, CCR2-positive nonneuronal cells present in L3, L5, and L6 DRG were counted by using the aforementioned DRG cryosections. The total number of CCR2-positive nonneuronal cells present in assayed tissue sections was divided by the number of neurons to arrive at a numerical ratio of CCR2-positive nonneuronal cells per neuron. Unbiased estimates of single-labeled MCP-1 DRG cell numbers were collected by using the same stereological analysis as described. The percentage of MCP-1/IB4-positive neurons was based on the numbers of MCP-1 positive neurons present in the tissue sections. Values are presented as means ± SEM. Numbers of cells generated in these assays were compared by using a two-tailed Student's unpaired *t* test assuming equal variances. A difference was accepted as significant if the probability was $<5\%$ ($P < 0.05$).

Cell-Size Frequency Histograms. Measurements of cross-sectional areas of neuronal cell profiles were performed by using the IMAGEPRO PLUS (Media Cybernetics, Silver Spring, MD) image analysis system. Digitized images collected for the neuronal cell counts were used for cell-size frequency histograms. For both CCR2 mRNA and MCP-1 immunoreactivity, all labeled neuronal profiles were measured in each section from four compressed L5 DRGs removed at POD5. To distinguish cell-size-specific changes, DRG neurons were characterized as small (<600 μm^2), medium-sized (600–1,200 μm^2), and large ($<1,200$ μm^2) neurons, according to their cross-sectional area (29, 30).

Electrophysiological Recording. Intracellular electrophysiological recordings in intact DRGs were obtained from 16 CCD rats 5–8 days after rod implantation and from eight unoperated control rats. Under pentobarbital anesthesia (50 mg/kg i.p.), the right L4 and L5 DRGs with their dorsal roots and peripheral connections to the sciatic nerve at the midthigh level were removed from the animal and transferred to a Petri dish containing artificial CSF (ACSF). The ACSF, containing (in mM) 130 NaCl, 24 $NaHCO_3$, 3.5 KCl, 1.25 NaH_2PO4, 1.2 $MgCl_2$, 1.2 $CaCl_2$, and 180 dextrose, was bubbled with 95% O_2 and 5% CO_2. The pH of the solution was 7.4, and the osmolarity, 290≈310 milliosmolar. After the perineurium and epineurium were peeled away from the ganglion, the preparation was placed in a recording chamber that was perfused continuously at a rate of 2–3 ml/min with oxygenated ACSF maintained at 36 ± 1°C by means of a servocontrolled in-line heater (Warner Instruments, Hamden, CT). The cut ends of the dorsal roots were inserted into suction electrodes for electrical stimulation. The intracellular recording electrode, fabricated from borosilicate glass (World Precision Instruments, Sarasota, FL) and pulled on a Flaming/Brown micropipette puller (P-97, Sutter Instruments, Novato, CA), was filled with 1 M KCl. Satisfactory recordings were obtained with electrodes of 60–80 MΩ for small DRG neurons and 40–60 MΩ for medium and large neurons.

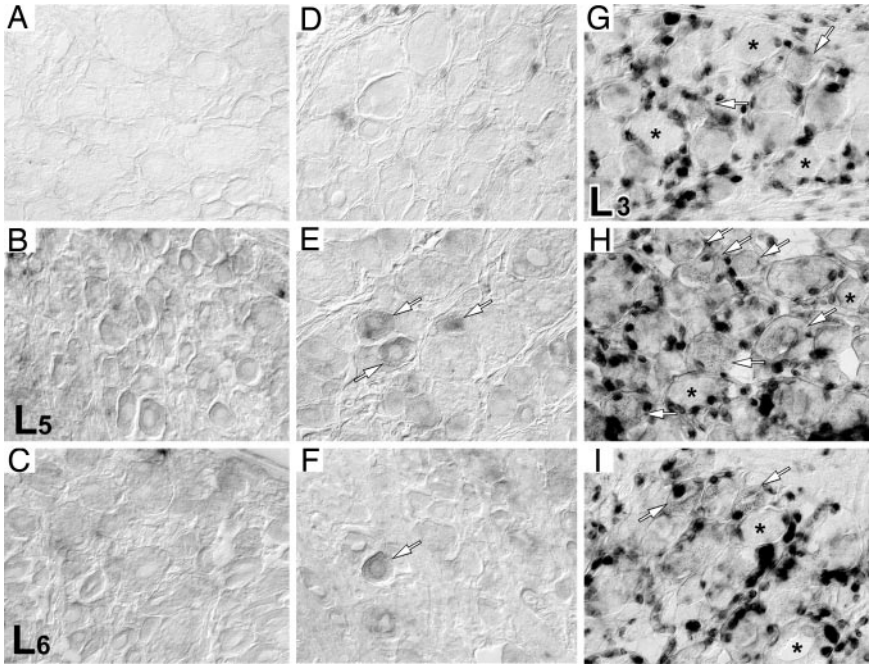

Fig. 1. CCR2 mRNA expression in compressed and adjacent noncompressed DRG at POD1, POD3, and POD5. (*A*) Sense riboprobe hybridization signal in representative compressed L5 DRG at POD5. (*B* and *C*) Compressed L5 DRG (*B*) and adjacent noncompressed L6 DRG (*C*) do not exhibit CCR2 mRNA expression at POD1. (*D*) Sham-treated L5 DRG expression levels of CCR2 mRNA at POD5. (*E* and *F*) Compressed L5 DRG (*E*) and adjacent noncompressed L6 (*F*) exhibit only neuronal CCR2 mRNA expression (white arrows) at POD3. (*G–I*) High levels of CCR2 mRNA are present in predominantly nonneuronal cells and some neurons (white arrows) of adjacent noncompressed L3 (*G*) and L6 (*I*) DRG at POD5. Compressed L5 DRG (*H*) at POD5 also exhibit high levels of CCR2 mRNA expression in predominantly nonneuronal cells, but many more neurons are positive for CCR2 mRNA transcripts (white arrows). Black asterisks indicate nonlabeled neurons (*G–I*). (Bar, 50 μm.)

Each recorded soma (cell body) was located on the surface of the DRG and viewed under differential interference contrast at $\times$40 by using a water immersion objective and upright microscope (BX50-WI, Olympus, Tokyo). The size of a DRG soma was classified according to its mean diameter (i.e., average of the longest and shortest diameters) as small ($\leq$30 μm), medium (31$\sim$45 μm), or large (>45 μm) (1, 27). In addition to somal size, neurons were categorized, in response to electrical stimulation of the dorsal root, by axonal conduction velocity and absence or presence of an inflection (hump) on the falling phase of the evoked action potential. The hump is characteristic of the action potentials of nociceptive neurons recorded *in vivo* (31, 32).

Only data from cells with a resting membrane potential equal to or more negative than $-$50 mV were accepted. Electrophysiological data were collected under current-clamp (MultiClamp 700A, Axon Instruments, Union City, CA), stored digitally via a Digidata 1320A interface (Molecular Devices), and analyzed offline with PCLAMP 8 software (Axon Instruments).

MCP-1 was purchased from R & D Systems. Lyophilized proteins were aliquoted in 0.1% BSA in PBS (BSA) and stored at $-$20°C for <3 weeks before use. A solution (100$\times$) was prepared just before experimentation. MCP-1 was diluted to the final concentration (100 nM) with the same oxygenated artificial CSF. The membrane potential was recorded for 1 min before, during, and after application of vehicle and then 1 min before, during, and after the application of MCP-1 in vehicle. The vehicle and MCP-1 were topically applied to the soma of each recorded neuron through a fast-switch pressure-controlled drug application system (Automate, Cranston, RI) with a 10-μm diameter tip. The tip was located $\approx$100 μm away from the neuron studied. To avoid possible tachyphylaxis caused by repeated applications of MCP-1, successive recorded neurons were located at least 200 μm away from each other.

Results

CCR2 mRNA Expression in Compressed and Adjacent Noncompressed DRG. Naïve (n = 3) and sham-operated DRG at POD5 (Fig. 1*D*) (n = 4) lacked CCR2 mRNA transcripts. Little to no CCR2 mRNA expression was present at POD1 or POD3 in assayed ganglia (L3–L6) (Fig. 1 *B* and *C*) with the exception of occasional neurons in compressed and noncompressed ganglia on POD3 (Fig. 1 *E* and *F*). Strong expression of CCR2 mRNA was observed at POD5 in nonneuronal cells of the compressed L5 ganglion (Fig. 1*H*) and in the adjacent ipsilateral ganglia L3 and L6 (Fig. 1 *G* and *I*). Neuronal expression was also present in L3 and L6 (Fig. 1 *G* and *I*) and more so in the compressed L5 (Fig. 1*H*). Compressed L4 DRG yielded CCR2 expression changes similar to compressed L5 (data not shown).

Stereological analysis of estimated cell numbers revealed that $\approx$33 $\pm$ 3.5%, 49 $\pm$ 6.2%, and 41 $\pm$ 5.6% of the L3, L5, and L6 DRG neurons were labeled for CCR2, respectively. Of particular interest, CCR2 mRNA transcripts were present in many small, medium, and large neurons in the compressed and ipsilateral/adjacent DRGs (Fig. 1 *G–I*). Data from a cell-size-frequency histogram revealed that most neurons in the compressed L5 DRG expressing CCR2 mRNA were of small and medium size on POD5 (Fig. 4*A*, which is published as supporting information on the PNAS web site). There was a statistical difference between the percentage of CCR2-positive neurons present in the noncompressed L3 DRG and compressed L5 DRG ($P < 0.05$), but statistical significance was not reached between compressed L5 and noncompressed L6 DRG.

A stereological analysis also revealed that the number of CCR2-positive nonneuronal cells per neuron was 2.11 $\pm$ 0.48 in L3 DRG, 5.33 $\pm$ 1.5 in L5 DRG, and 2.81 $\pm$ 0.74 in L6 DRG (n = 4). There was a statistical difference between the ratios of CCR2-positive nonneuronal cells to neurons present in compressed and noncompressed ganglia ($P < 0.05$). These cells were

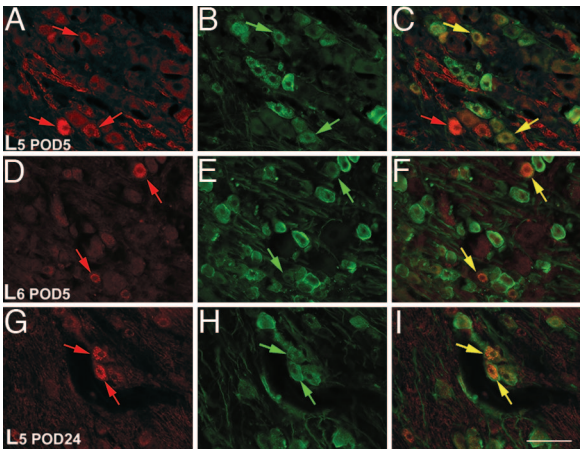

Fig. 2. MCP-1 immunoreactivity and isolectin B4 binding in compressed lumbar DRG 5 (L5) and adjacent noncompressed L6 DRG at POD5 and in compressed L5 ganglia at POD24. (*A*, *D*, and *G*) MCP-1 immunoreactivity (red arrows) in (*A*) L5 and (*D*) L6 DRG at POD5, and (*G*) L5 DRG at POD24. (*B*, *E*, and *H*) Isolectin B4 binding (green arrows) in compressed L5 (*B*) and adjacent noncompressed L6 DRG (*E*) at POD5 and in compressed L5 DRG (*H*) at POD24. (*C*, *F*, and *I*) Merged images of MCP-1 (red arrows) and IB4 (green arrows) and colocalization (yellow arrows) at POD5 (*C* and *F*) and POD24 (*I*). (Bars, 100 μm.)

typically found adjacent to neuronal somata of all sizes, regardless of the presence or absence of neuronal CCR2 mRNA expression. Expression of CCR2 mRNA by nonneuronal cells was not absolute, because some nonneuronal cells did not exhibit CCR2 mRNA (Fig. 1 *G–I*).

Macrophage Infiltration of Compressed and Adjacent Ganglia. The chemokine receptor CCR2 is commonly associated with monocytes and macrophages. To determine the degree to which macrophages contribute to the number of nonneuronal CCR2-positive cells, we examined L3–L6 DRG tissue sections taken from naïve, sham, and CCD animals at POD5 for the presence of ED-1 (a marker of rat macrophages). Sham-treated and naïve DRGs exhibited few ED-1-positive cells (data not shown). Similar to sham-treated and naïve DRG, adjacent noncompressed L3 (data not shown) and L6 ganglia at POD5 exhibited few ED-1-positive cells (Fig. 5*B*, which is published as supporting information on the PNAS web site). Compressed L4/L5 ganglia displayed numerous ED-1-positive cells at POD5 (Fig. 5*A*).

Cellular Localization of MCP-1 Protein Synthesis. Having found that CCD injury up-regulated CCR2 in both compressed and ipsilateral/adjacent DRGs, we examined these ganglia for a source of MCP-1, the most common chemokine ligand for CCR2. MCP-1 was not detectable in the DRGs of naïve or sham-treated animals at POD5 or in DRGs subjected to CCD injury at POD1 or POD3 (data not shown). At POD5, MCP-1 immunoreactivity was clearly present in many cell bodies of compressed L5 DRG (Fig. 2*A*). MCP-1-immunopositive neurons made up 28.63 ± 2.23% of the total number of neurons counted in the compressed L5 DRG. Adjacent noncompressed L3 (data not shown) and L6 DRG also exhibited MCP-1 immunoreactive cell bodies at POD5 (Fig. 2*D*). The percentage of MCP-1 immunopositive neurons present in L3 and L6 DRG at POD5 were 18.54 ± 3.18% and 24.67 ± 5.22%, respectively. The percentage of MCP-1 immunopositive neurons present in the compressed L5 DRG at POD5 was greater than that in the adjacent noncompressed L3 DRG ($P < 0.05$) but not significantly different from the percentage present in L6 DRG.

Some MCP-1 immunoreactive neurons also bound the lectin IB4, a marker of small nonpeptidergic nociceptive neurons (Fig. 2 *C* and *F*). A significant proportion of MCP-1-positive neurons in the compressed L5 and noncompressed L6 DRGs also expressed IB4 (43.54 ± 8.62% and 77.56 ± 12.06%, respectively) at POD5. Neurons exhibiting MCP-1 immunoreactivity persisted in the L4/L5 DRGs through POD24 ($n = 2$, the latest timepoint examined; Fig. 2*G*). Cell-size-frequency histograms of L5 CCD DRGs revealed that small and medium-sized neurons were MCP-1 immunoreactive at POD5 (Fig. 4*B*). By POD24, most MCP-1 immunoreactivity was limited to small neurons that almost completely colocalized with neurons that bound the lectin IB4 (Fig. 2*I*). MCP-1 immunoreactivity was not detectable in nonneuronal cells in either injured or adjacent noncompressed DRGs at POD5 and -24.

MCP-1 Excites Injured Sensory Neurons. Because CCD DRG neurons up-regulated both CCR2 and its agonist, MCP-1, we examined the effects of MCP-1 on the excitability of neurons in the intact DRG. Electrophysiological recordings were compared for compressed DRGs from CCD rats and noncompressed DRGs from naïve (unoperated)-control rats. MCP-1 exhibited a powerful excitatory effect almost entirely confined to CCD DRG neurons, whereas its vehicle alone evoked no significant responses. A total of 20 small (10 CCD and 10 control), 30 medium (17 CCD and 13 control), and 20 large neurons (10 CCD and 10 control) were studied. MCP-1 depolarized (≥2 mV) only 2 of 33 control DRG neurons (6%). In contrast, 25 of 37 CCD neurons (68%) responded to MCP-1 with a mean depolarization

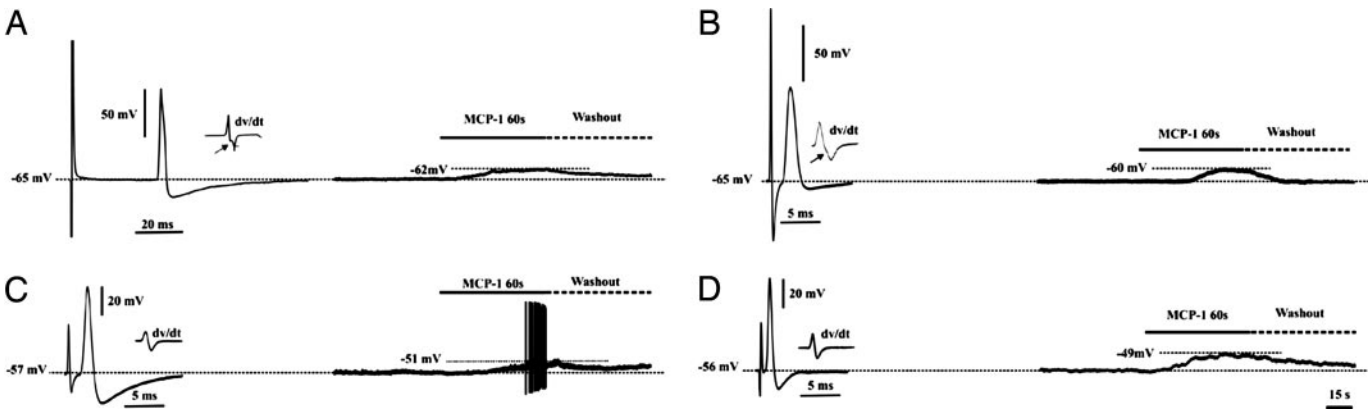

Fig. 3. Responses of DRG neurons to MCP-1 applied to somata on the surface of the formerly compressed ganglion at POD5. The neurons were classified visually by somal size as small (*A*), medium (*B* and *C*), or large (*D*). Each neuron was further classified by axonal conduction velocity (action potential proceeded by artifact electrically evoked from dorsal root, on the left) and by the presence or absence of a "hump" on the falling phase of the action potential causing an extra deflection in the first derivative (arrows, *A* and *B Left Inset*). The hump is typical for nociceptive neurons.

of 4.7 ± 0.94 mV (range of 2.1 to 15.1 mV) (Fig. 3). Thus, CCD neurons were much more likely to respond to MCP-1 than control neurons ($P \leq 0.001$, χ^2 test). Two large- and two small-sized CCD neurons exhibited action potential discharges during the application of MCP-1 (Fig. 3*C*). The discharges ceased and the changes in the membrane potential reversed partially or completely within 1 min of the washout of MCP-1. The proportions of responsive small-, medium-, and large-sized CCD neurons were 6/10, 12/17, and 7/10, respectively. Responsive CCD neurons included 7 classified as nociceptive and 18 as nonnociceptive, according to the presence or absence, respectively, of an inflection on the falling phase of the action potentials electrically evoked by stimulation of the dorsal root (Fig. 3). Thus, MCP-1 was interpreted as exciting subpopulations of both nociceptive and nonnociceptive neurons.

Discussion

The present findings demonstrate that a chronic compression of the DRG induces neuronal expression of the chemokine receptor CCR2 mRNA and its preferred ligand, MCP-1. Significantly, these changes occur in both compressed DRGs and noncompressed ("uninjured") adjacent DRGs. Furthermore, we provide a cellular mechanism that may contribute to the hyperexcitability of sensory neurons and thus pain behavior in this model: both nociceptive and nonnociceptive neurons become responsive to MCP-1 after CCD. Because most neurons tested in the compressed DRG were responsive to MCP-1 after CCD injury, *in situ* release of MCP-1 may contribute to the neuronal hyperexcitability in a cellular autonomous or paracrine manner.

Previous studies have proposed a role of chemokines in exciting nociceptive primary sensory neurons. Dissociated embryonic DRG neurons with nociceptive properties express the receptors for, and are excited by, a variety of chemokine receptors (2). Moreover, attenuation of pain hypersensitivity after injury was described in null mutant CCR2 mice (3). However, neither study addressed the role of MCP-1/CCR2 signaling in the context of chronic pain *in vivo*. The present study demonstrates that there is a neuronal up-regulation of CCR2 gene expression that is concurrent with the up-regulation of MCP-1 protein after a chronic compression injury. Although the onset of these neuronal changes does not coincide with the initiation of tactile allodynia and hyperalgesia in the CCD injured rat, they may be central to the chronic nature of certain neuropathic pain behaviors. Moreover, we find that neurons in the formerly compressed intact DRG develop an excitatory response to MCP-1 that they normally do not exhibit. These results suggest that some of the modifications of these electrophysiological events associated with neuropathic pain behaviors are likely because of the combination of inflammation-induced neuronal production of the MCP-1 and CCR2 and MCP-1/CCR2 signaling.

Despite the acute axotomy necessitated by the preparation, the active and passive membrane properties recorded from neuronal somata from the intact DRG *in vitro* are very similar or identical to those obtained *in vivo* (1). Moreover, recent patch–clamp studies demonstrated that the capacity of MCP-1 to depolarize DRG neurons after CCD is an intrinsic property of the neuron, i.e., is retained after the cell bodies are acutely dissociated.** Under current clamp, MCP-1 evoked a dose-dependent inward current with an EC_{50} of 52 nM. Further analyses in voltage clamp mode indicated that the depolarization of DRG neurons by MCP-1 is mediated by a nonspecific cation conductance.

Regulation of MCP-1 in Injured Neurons. MCP-1 immunoreactivity has previously been observed in injured neurons after the transection of axons of sensory, sympathetic, and facial motor neurons (21, 22, 34). The expression of MCP-1 is induced within hours of the injury. In contrast, our results demonstrate a time course of CCD-induced neuronal MCP-1 expression that does not appear until POD5 and lasts at least as long as POD24. This time course may reflect an association with the chronic aspects of the long-lasting pain behavior and cutaneous hyperalgesia (e.g., ref. 46). CCD injury-induced expression of neuronal MCP-1, as described here, presumably requires the activation of a signaling cascade of cytokines and other mediators upstream of MCP-1/CCR2 expression. Possible candidates are TNF-α (35, 36), IL-6, and leukemia inhibitory factor (23). In addition, neuronal chemokine production may be regulated by NMDA-mediated signaling produced by peripheral nerve injury (37).

After a transection or crush of a peripheral nerve, there is a rapid increase in MCP-1 immunoreactive Schwann cells (36, 38) at the injury site. This glial chemokine expression is followed at the site of injury by MCP-1-positive macrophages, fibroblast-like cells, and endothelial cells (38). In contrast, our results do not demonstrate an increase of MCP-1 in glia or other nonneuronal cells in the compressed or adjacent noncompressed DRG.

MCP-1 binding to CCR2 receptors on nonneuronal cells may also contribute to the excitatory effects on neurons via an indirect route (i.e., release of TNF-α or IL-1β) by satellite cells or macrophages (39, 40). However, these actions are unlikely to account for the excitatory effects of MCP-1 on electrophysiological responses of sensory neurons, because such effects persist (and are slightly larger in magnitude) in dissociated adult DRG neurons that are superfused to wash away possible substances released from nonneuronal cells.** Taken together, these results suggest that some of the modifications of these electrophysiological events are likely because of the combination of a CCD-induced neuronal production of MCP-1 and CCR2.

Gene Expression Changes in the Adjacent Noncompressed Ganglia. There are several possible mechanisms by which a compression of the L4 and L5 ganglia might lead to up-regulation of CCR2 in the adjacent noncompressed DRGs. One possibility is that the implanted rods cause an inflammation of the dura and the release of cytokines from activated immune cells known to be present in the dura (41). These cytokines or those released by cells in the injured DRGs that enter the CSF might activate cells in the adjacent ganglia.

Cytokines might also be released from activated microglia and astrocytes in the spinal cord dorsal horn after chronic activity in injured DRG afferent neurons (42, 43). These spinal cord-derived cytokines may directly signal both the injured and uninjured lumbar DRG neurons through receptors present on primary afferent central terminations (44). This signaling via primary sensory neuron central terminations is not unique to cytokines. Romero *et al.* (45), by using conditional overexpression of nerve growth factor (NGF) in the adult spinal cord, demonstrated that a subpopulation of tyrosine kinase A (TrkA) positive nociceptive primary afferent neurons is capable of robust central axon plasticity after exposure to spinal cord-derived sources of NGF. More recent data demonstrate that lumbrosacral DRGs some distance from a thoracic spinal cord injury exhibit a persistent inflammatory response involving macrophages and T lymphoctyes (46). This inflammatory response in the lumbar DRGs may be driven by neuronal signals derived from exposure of receptor-bearing primary afferent central terminals to cytokines, glutamate, and/or growth factors.

In addition, the central effects of sustained activation of nociceptive neurons in the compressed DRG might produce a centrally mediated chronic abnormal nerve impulse activity in the adjacent noncompressed DRGs. Nociceptive input to the spinal cord that is peripherally generated via one dorsal root can elicit dorsal root reflexes, i.e., centrally mediated antidromic action potentials in an adjacent dorsal root (47). Taken together, the presence of cytokines

**Sun, J., Yang, B., Ma, C., Donnelly, D. F. & LaMotte, R. H. (2005) *Soc. Neurosci. Abstr.*, 511.15 (abstr.).

and/or chronic abnormal nerve impulse activity could then activate second messenger and nuclear transcription factors in adjacent uninjured DRG effectively up-regulating CCR2.

Chemokine Receptor Signaling in Neurons. Our data indicate that MCP-1 rapidly modulates DRG neuronal response, demonstrating a peripheral MCP-1 action on nociceptive and nonnociceptive signaling. The rapid effects of MCP-1 are likely mediated through its cognate G protein-coupled receptor, CCR2, and act on various intracellular signaling cascades including phospholidase C (PLC). MCP-1/CCR2 activation induces the dissociation of $G\alpha_i$ and $G\beta\gamma$ subunits from trimeric G proteins, in turn stimulating PLC activity. PLC hydrolyzes inositol phospholipid 2 (PIP2) into membrane-bound diacylglycerol and soluble inositol triphosphate (IP_3). Generation of IP_3 results in inositol triphosphate receptor-mediated release of Ca^{2+} from intracellular stores and Ca^2 influx. This signaling pathway might be a key element in sensory neuron excitation and resulting pain (48).

Interestingly, inositol phospholipid 2 (PIP2), which is situated on the inner leaflet of the cell membrane, tonically blocks transient receptor potential (TRP)V1 channels (49). TRPV1 is the receptor for capsaicin, the irritant pain-producing substance that is synthesized by hot peppers (50). After hydrolysis of PIP2, TRPV1 is unblocked, allowing Na^+ entry down its electrochemical gradient and depolarization of the neuron (49). A recent publication demonstrates that activation of CCR1 receptors expressed by DRG neurons produces transactivation of the TRPV1 receptor by the same pathway (51).

The release of $G\beta\gamma$ subunits from trimeric G proteins can also result in stimulation of ERK1/2, JNK, and p38 mitogen-activated protein kinases (MAPKs). The activation of MAPK by MCP-1 has been reported in different kinds of cells (52–55), and we recently observed an up-regulation of pERK in CCD neurons (unpublished data). In addition, an activation of MAPK has been shown to inhibit K^+ conductances in nociceptive neurons (56). Thus, it is possible that MCP-1/CCR2 signaling might modulate neuronal excitability via the activation of MAPK in DRG neurons.

A state of abnormal neuronal excitability and "chronic inflammation" of DRG neurons leading to the novel expression of CCR2 receptors is likely to contribute to pain behavior. Possibly the antagonism of CCR2 receptors could furnish a novel therapeutic approach to diminishing the chronic inflammatory state and the evoked neuropathic pain behaviors that accompany it. Our results further illustrate the role of chemokines as mediators of pathophysiological phenomena within the adult nervous system.

We greatly appreciate the assistance of Ken Greenquist. This research was supported by an Illinois Excellence in Medicine grant (to F.A.W.), the National Multiple Sclerosis Society (to F.A.W.), and the National Institutes of Health [Grants NS014624 and NS038317 (to R.H.L.) and DA013141, NS043095, and MH040165 (to R.J.M.)].

1. Ma, C., Shu, Y., Zheng, Z., Chen, Y., Yao, H., Greenquist, K. W., White, F. A. & LaMotte, R. H. (2003) *J. Neurophysiol.* **89,** 1588–1602.
2. Oh, S. B., Tran, P. B., Gillard, S. E., Hurley, R. W., Hammond, D. L. & Miller, R. J. (2001) *J. Neurosci.* **21,** 5027–5035.
3. Abbadie, C., Lindia, J. A., Cumiskey, A. M., Peterson, L. B., Mudgett, J. S., Bayne, E. K., DeMartino, J. A., MacIntyre, D. E. & Forrest, M. J. (2003) *Proc. Natl. Acad. Sci. USA* **100,** 7947–7952.
4. Waters, S. M., Steflik, J., Cortright, D. N., Ma, C., LaMotte, R. H. & White, F. A. (2004) *Soc. Neurosci. Abstr.* **31,** 64.4.
5. Charo, I. F., Myers, S. J., Herman, A., Franci, C., Connolly, A. J. & Coughlin, S. R. (1994) *Proc. Natl. Acad. Sci. USA* **91,** 2752–2756.
6. Charo, I. F. & Peters, W. (2003) *Microcirculation* **10,** 259–264.
7. Babcock, A. A., Kuziel, W. A., Rivest, S. & Owens, T. (2003) *J. Neurosci.* **23,** 7922–7930.
8. Kuziel, W. A., Morgan, S. J., Dawson, T. C., Griffin, S., Smithies, O., Ley, K. & Maeda, N. (1997) *Proc. Natl. Acad. Sci. USA* **94,** 12053–12058.
9. Lu, B., Rutledge, B. J., Gu, L., Fiorillo, J., Lukacs, N. W., Kunkel, S. L., North, R., Gerard, C. & Rollins, B. J. (1998) *J. Exp. Med.* **187,** 601–608.
10. Tran, P. B. & Miller, R. J. (2003) *Nat. Rev. Neurosci.* **4,** 444–455.
11. Banisadr, G., Queraud-Lesaux, F., Boutterin, M. C., Pelaprat, D., Zalc, B., Rostene, W., Haour, F. & Parsadaniantz, S. M. (2002) *J. Neurochem.* **81,** 257–269.
12. Andjelkovic, A. V., Kerkovich, D., Shanley, J., Pulliam, L. & Pachter, J. S. (1999) *Glia* **28,** 225–235.
13. Andjelkovic, A. V. & Pachter, J. S. (2000) *J. Neurochem.* **75,** 1898–1906.
14. Ji, J. F., He, B. P., Dheen, S. T. & Tay, S. S. (2004) *Neurosci. Lett.* **355,** 236–240.
15. Tran, P. B., Ren, D., Veldhouse, T. J. & Miller, R. J. (2004) *J. Neurosci. Res.* **76,** 20–34.
16. Horuk, R. (2001) *Cytokine Growth Factor Rev.* **12,** 313–335.
17. Rot, A. & von Andrian, U. H. (2004) *Annu. Rev. Immunol.* **22,** 891–928.
18. Rossi, D. & Zlotnik, A. (2000) *Annu. Rev. Immunol.* **18,** 217–242.
19. Biber, K., Zuurman, M. W., Homan, H. & Boddeke, H. W. (2003) *J. Leukocyte Biol.* **74,** 243–251.
20. Fra, A. M., Locati, M., Otero, K., Sironi, M., Signorelli, P., Massardi, M. L., Gobbi, M., Vecchi, A., Sozzani, S. & Mantovani, A. (2003) *J. Immunol.* **170,** 2279–2282.
21. Tanaka, T., Minami, M., Nakagawa, T. & Satoh, M. (2004) *Neurosci. Res.* **48,** 463–469.
22. Schreiber, R. C., Krivacic, K., Kirby, B., Vaccariello, S. A., Wei, T., Ransohoff, R. M., Zigmond, R. E. (2001) *NeuroReport* **12,** 601–606.
23. Tofaris, G. K., Patterson, P. H., Jessen, K. R. & Mirsky, R. (2002) *J. Neurosci.* **22,** 6696–6703.
24. Ueda, A., Okuda, K., Ohno, S., Shirai, A., Igarashi, T., Matsunaga, K., Fukushima, J., Kawamoto, S., Ishigatsubo, Y. & Okubo, T. (1994) *J. Immunol.* **153,** 2052–2063.
25. Hu, S. J. & Xing, J. L. (1998) *Pain* **77,** 15–23.
26. Song, X. J., Hu, S. J., Greenquist, K. W., Zhang, J. M. & LaMotte, R. H. (1999) *J. Neurophysiol.* **82,** 3347–3358.
27. Zhang, J. M., Song, X. J. & LaMotte, R. H. (1999) *J. Neurophysiol.* **82,** 3359–3366.
28. West, M. J. (1999) *Trends Neurosci.* **22,** 51–61.
29. Fukuoka, T., Tokunaga, A., Tachibana, T., Dai, Y., Yamanaka, H. & Noguchi, K. (2002) *Pain* **99,** 111–120.
30. Schafers, M., Geis, C., Svensson, C. I., Luo, Z. D. & Sommer, C. (2003) *Eur. J. Neurosci.* **17,** 791–804.
31. Djouhri, L. & Lawson, S. N. (2001) *Neuroscience* **108,** 479–491.
32. Koerber, H. R., Druzinsky, R. E. & Mendell, L. M. (1988) *J. Neurophysiol.* **60,** 1584–1596.
33. Sun, J. H., Ma, C., Tan, Z., White, F. A., Miller, R. J. & LaMotte, R. H. (2004) *Soc. Neurosci. Abstr.* **31,** 64.6.
34. Flugel, A., Hager, G., Horvat, A., Spitzer, C., Singer, G. M., Graeber, M. B., Kreutzberg, G. W. & Schwaiger, F. W. (2001) *J. Cereb. Blood Flow Metab.* **21,** 69–76.
35. Glabinski, A. R., Bielecki, B., Kolodziejski, P., Han, Y., Selmaj, K. & Ransohoff, R. M. (2003) *J. Interferon Cytokine Res.* **23,** 457–466.
36. Subang, M. C. & Richardson, P. M. (2001) *Eur. J. Neurosci.* **13,** 521–528.
37. Kleinschnitz, C., Brinkhoff, J., Zelenka, M., Sommer, C. & Stoll, G. (2004) *J. Neuroimmunol.* **149,** 77–83.
38. Taskinen, H. S. & Roytta, M. (2000) *J. Peripher. Nerv. Syst.* **5,** 75–81.
39. Ohtori, S., Takahashi, K., Moriya, H. & Myers, R. R. (2004) *Spine* **29,** 1082–1088.
40. Sekiguchi, M., Kikuchi, S. & Myers, R. R. (2004) *Spine* **29,** 1105–1111.
41. McMenamin, P. G. (1999) *J. Comp. Neurol.* **405,** 553–562.
42. Watkins, L. R., Martin, D., Ulrich, P., Tracey, K. J. & Maier, S. F. (1997) *Pain* **71,** 225–235.
43. DeLeo, J. A. & Yezierski, R. P. (2001) *Pain* **90,** 1–6.
44. Holmes, G. M., Hebert, S. L., Rogers, R. C. & Hermann, G. E. (2004) *Brain Res.* **1025,** 210–219.
45. Romero, M. I., Rangappa, N., Li, L., Lightfoot, E., Garry, M. G. & Smith, G. M. (2000) *J. Neurosci.* **20,** 4435–4445.
46. McKay, S. M. & McLachlan, E. M. (2004) *NeuroReport* **15,** 1783–1786.
47. Lin, Q., Zou, X. & Willis, W. D. (2000) *J. Neurophysiol.* **84,** 2695–2698.
48. Oh, S. B., Endoh, T., Simen, A. A., Ren, D. & Miller, R. J. (2002) *J. Neuroimmunol.* **123,** 66–75.
49. Chuang, H.-h., Prescott, E. D., Kong, H., Shields, S., Jordt, S.-E., Basbaum, A. I., Chao, M. V. & Julius, D. (2001) *Nature* **411,** 957–962.
50. Julius, D. & Basbaum, A. I. (2001) *Nature* **413,** 203–210.
51. Zhang, N., Inan, S., Cowan, A., Sun, R., Wang, J. M., Rogers, T. J., Caterina, M. & Oppenheim, J. J. (2005) *Proc. Natl. Acad. Sci. USA* **102,** 4536–4541.
52. Kim, S. Y., Bae, J. C., Kim, J. Y., Lee, H. L., Lee, K. M., Kim, D. S. & Cho, H. J. (2002) *NeuroReport* **13,** 2483–2486.
53. Sodhi, A. & Biswas, S. K. (2002) *J. Interferon Cytokine Res.* **22,** 517–526.
54. Jimenez-Sainz, M. C., Fast, B., Mayor, F., Jr., & Aragay, A. M. (2003) *Mol. Pharmacol.* **64,** 773–782.
55. Ogilvie, P., Paoletti, S., Clark-Lewis, I. & Uguccioni, M. (2003) *Blood* **102,** 789–794.
56. Hu, H. J. & Gereau, R. W. t. (2003) *J. Neurophysiol.* **90,** 1680–1688.